Title

Novel VCP mutations in inclusion body myopathy associated with Paget disease of bone and frontotemporal dementia

Journal

Clinical Genetics, 72(5)

ISSN

0009-9163

Authors

Watts, GDJ
Thomasova, D
Ramdeen, SK
et al.

Publication Date

2007-11-01

DOI

10.1111/j.1399-0004.2007.00887.x

Clin Genet 2007: 72: 420–426
Printed in Singapore. All rights reserved

CLINICAL GENETICS
doi: 10.1111/j.1399-0004.2007.00887.x

Original Article

Novel VCP mutations in inclusion body myopathy associated with Paget disease of bone and frontotemporal dementia

Watts GDJ, Thomasova D, Ramdeen SK, Fulchiero EC, Mehta SG, Drachman DA, Weihl CC, Jamrozik Z, Kwiecinski H, Kaminska A, Kimonis VE. Novel VCP mutations in inclusion body myopathy associated with Paget disease of bone and frontotemporal dementia. Clin Genet 2007: 72: 420–426. © Blackwell Munksgaard, 2007

Inclusion body myopathy associated with Paget disease of bone and frontotemporal dementia (IBMPFD, OMIM 167320) has recently been attributed to eight missense mutations in valosin-containing protein (VCP). We report novel VCP mutations N387H and L198W in six individuals from two families who presented with proximal muscle weakness at a mean age of diagnosis of 40 years, most losing the ability to walk within a few years of onset. Electromyographic studies in four individuals were suggestive of 'myopathic' changes, and neuropathic pattern was identified in one individual in family 1. Muscle biopsy in four individuals showed myopathic changes characterized by variable fiber size, two individuals showing rimmed vacuoles and IBM-type cytoplasmic inclusions in muscle fibers, and electron microscopy in one individual revealing abundant intranuclear inclusions. Frontotemporal dementia associated with characteristic behavioral changes including short-term memory loss, language difficulty, and antisocial behavior was observed in three individuals at a mean age of 47 years. Detailed brain pathology in one individual showed cortical degenerative changes, most severe in the temporal lobe and hippocampus. Abundant ubiquitin-positive tau-, α-synuclein-, polyglutamine repeat-negative neuronal intranuclear inclusions and only rare intracytoplasmic VCP positive inclusions were seen. These new mutations may cause structural changes in VCP and provide some insight into the functional effects of pathogenic mutations.

GDJ Watts[a]*, D Thomasova[a]*, SK Ramdeen[a]*, EC Fulchiero[a], SG Mehta[a], DA Drachman[b], CC Weihl[c], Z Jamrozik[d], H Kwiecinski[d], A Kaminska[d] and VE Kimonis[a]

[a]Division of Genetics, Children's Hospital Boston, Harvard Medical School, Boston, MA, USA, [b]Departments of Pathology and Neurology, University of Massachusetts Medical School, Worcester, MA, USA, [c]Department of Neurology, Washington University School of Medicine, Saint Louis, MO, USA, and [d]Department of Neurology, Medical University of Warsaw, Warsaw, Poland

*These authors contributed equally to this work.

Key words: chromosome 9p13.3-12 – frontotemporal dementia – hereditary inclusion body myopathy – limb-girdle muscular dystrophy – Paget disease of bone – Valosin-containing protein

Corresponding author: Virginia E. Kimonis, MD, MRCP, Department of Pediatrics, Division of Genetics and Metabolism, University of California, Irvine, 101 The City Drive, ZOT 4482, Orange, CA 92868, USA.
Tel.: +1 714 456 5791;
fax: +1 714 456 5330;
e-mail: vkimonis@uci.edu

Received 7 May 2007, revised and accepted for publication 10 July 2007

Hereditary inclusion body myopathy associated with Paget disease of bone (PDB) and frontotemporal dementia (FTD) (IBMPFD, OMIM 167320) is a progressive autosomal dominant disorder that manifests as one or a combination of its disease phenotypes (1, 2) attributed to missense mutations in valosin-containing protein (VCP, p97, CDC48, MIM 601023) by Watts et al. (3). VCP is a member of the Type II AAA-ATPase family that has been associated with a number of essential cellular processes, including membrane fusion, nuclear envelope reconstruction and post-mitotic Golgi reassembly and ubiquitin-dependent protein degradation, among others (4–6). VCP exists as a barrel-like homohexamer made of two ring-shaped layers that create a complex interior core (7). Watts et al. (3) identified and described six missense mutations in VCP that cause

IBMPFD: p.R95G, p.R155H, p.R155C, p.R155P located within the ubiquitin and cofactor binding N-terminal domain, p.R191Q within the linker connecting N and D1 domains, and p.A232E within the D1-ATPase domain. Two more IBMPFD associated VCP mutations were identified recently in European families: p.R93C and p.R159H (8, 9).

Patients, materials and methods

Informed consent was obtained for this study as approved by Children's Hospital Boston, MA, USA. Clinical evaluations, review of records, analysis of serum alkaline phosphatase (AP), creatine kinase (CK), X-rays and muscle biopsies were obtained. Medical records of deceased individuals were reviewed. Clinical features of seven individuals from two unrelated families are summarized in Table 1 and Table 2.

Family 1

In family 1, from Poland as shown in Fig. 1(**a**), two siblings suffered from progressive myopathy. One of the siblings displayed early stages of dementia associated with brain computed tomographic (CT) changes of cortical and subcortical cerebral atrophy. No individual was diagnosed with PDB.

Case 1

Individual 1-1, a member of a family, is a 54-year-old man with a 7-year history of muscle weakness of the shoulders and arms, and he had difficulty getting up from the chair. Clinical examination identified marked proximal weakness and wasting of the upper and lower extremities and mild lumbar hyperlordosis. Scapular winging and quadriceps muscle involvement was noted. At the age of 53 years, he lost the ability to walk unaided.

Case 2

Individual 1-2, a 47-year-old man, the younger of the affected siblings, had a 3-year history of increasing weakness of the arms and legs. On examination, mild atrophy and weakness of shoulders and arms with winging of the scapulae and advanced atrophy of quadriceps muscles and prominent calves were noted. Brain CT showed marked diffuse cortical and subcortical brain atrophy, and psychometric tests revealed an IQ of 99 and mild recent memory deficit.

Muscle biopsy of the vastus lateralis showed advanced 'myopathic' changes with variable fiber sizes and fiber splitting in both individuals. Eosinophilic inclusions were visible in hematoxylin and eosinophil staining in some fibers [Fig. 1(**c**)], and many fibers contained single or multiple vacuoles rimmed by small basophilic granules [Fig. 1(**d**)]. Electron microscopy revealed multiple IBM-type tubulofilamentous inclusions and a variety of nonspecific cytoplasmic changes including vacuolation, myelin figures and cytoplasmic bodies [Fig. 1(**f–h**)]. IBM-type inclusions composed of randomly oriented tubulofilaments 15–21 nm in diameter were abundant in the muscle nuclei and rarely seen in the cytoplasm. Many nuclei were broken down, and the inclusions liberated into the cytoplasm.

Case 3

Individual 1–3 the mother of the two siblings died at age 52 years. Autopsy was not performed, and medical records were not available. In the last 6 years of her life, however, she developed odd, antisocial behavior and progressive dementia. Psychological tests and CT apparently diagnosed her with sporadic 'Pick disease'.

Family 2

Although this North American family of non-Jewish ancestry is large [Fig. 1(**b**)], only the proband was available for examination. Medical

Table 1. Clinical data of affected individuals

Family	Individual	Age[a] (years)	Deceased	Sex	Myopathy	PDB	Dementia	Age diagnosis myopathy (years)	Age diagnosis PDB (years)	Age diagnosis dementia (years)
1	1–1[b]	54	–	M	+	–	–	48	–	–
	1–2	47	–	M	+	–	+	44	–	46
	1–3	52	+	F	–	–	+	–	–	46
2	2–1[b]	36	–	F	+	–	–	35	–	–
	2–2	52	+	M	+	+	+	37	49	50
	2–3	58	+	M	+	–	–	43	–	–
	2–4	57	+	M	+	+	–	35	44	–

F, female; M, male; PDB, Paget disease of bone.
[a]Indicates current age or age when deceased.
[b]Indicates proband.

Table 2. Laboratory data on affected individuals

Family	Individual	AP (U/l)	CK (U/l)	EMG	Muscle biopsy	Affected muscle areas	PDB location	FTD findings
1	1–1	Normal	Normal	Myopathic	Vastus lateralis: Myopathic, varied fiber size, rimmed vacuoles, inclusions	Shoulders, arms, legs, scapular winging	n/a	n/a
	1–2	Normal	95[a]	Mixed myopathic-neurogenic	Vastus lateralis: Myopathic, atrophic type I fibers, rimmed vacuoles	Shoulders, arms, quadriceps	n/a	Diffuse cortical and subcortical brain atrophy, mild memory deficiency
	1–3	n/a	n/a	n/a	n/a	n/a	n/a	Odd, antisocial behavior, clinical diagnosis of Pick's disease
2	2–1	59	473	Myopathic	Deltoid: Myopathic, varied fiber size, rimmed vacuoles	Right arm, posterior paraspinal group, multifidus, semispinalis, scapular winging	n/a	n/a
	2–2	782	62	NA	Quadriceps and PM: Myopathic, varied fiber size, atrophic fibers, rimmed vacuoles, cytoplasmic inclusions	Arms, legs, scapular winging	Bone scan: L2 vertebral body, right innominate bone, skull frontal bones	Cortical degenerative changes, mild memory loss, significant language difficulty, increased hostility
	2–3	n/a	n/a	NA	NT	Neck, back, shoulder girdle, arms, forearms, hands, pelvic girdle, legs	n/a	n/a
	2–4	n/a	n/a	Myopathic irritative	NA	Arms and legs	Spine, pelvis	n/a

EMG, electromyographic; FTD, frontotemporal dementia; n/a, not applicable; NA, not available; NT, not tested; PDB, Paget disease of bone; PM, postmortem. Myopathic, small amplitude, brief polyphasic action potentials present. Irritative, spontaneous fibrillations or positive sharp waves present. Normal values: AP 30–120 U/l, CK $<$ 200 U/l.
[a]On a different scale with normal values 0–34 U/l.

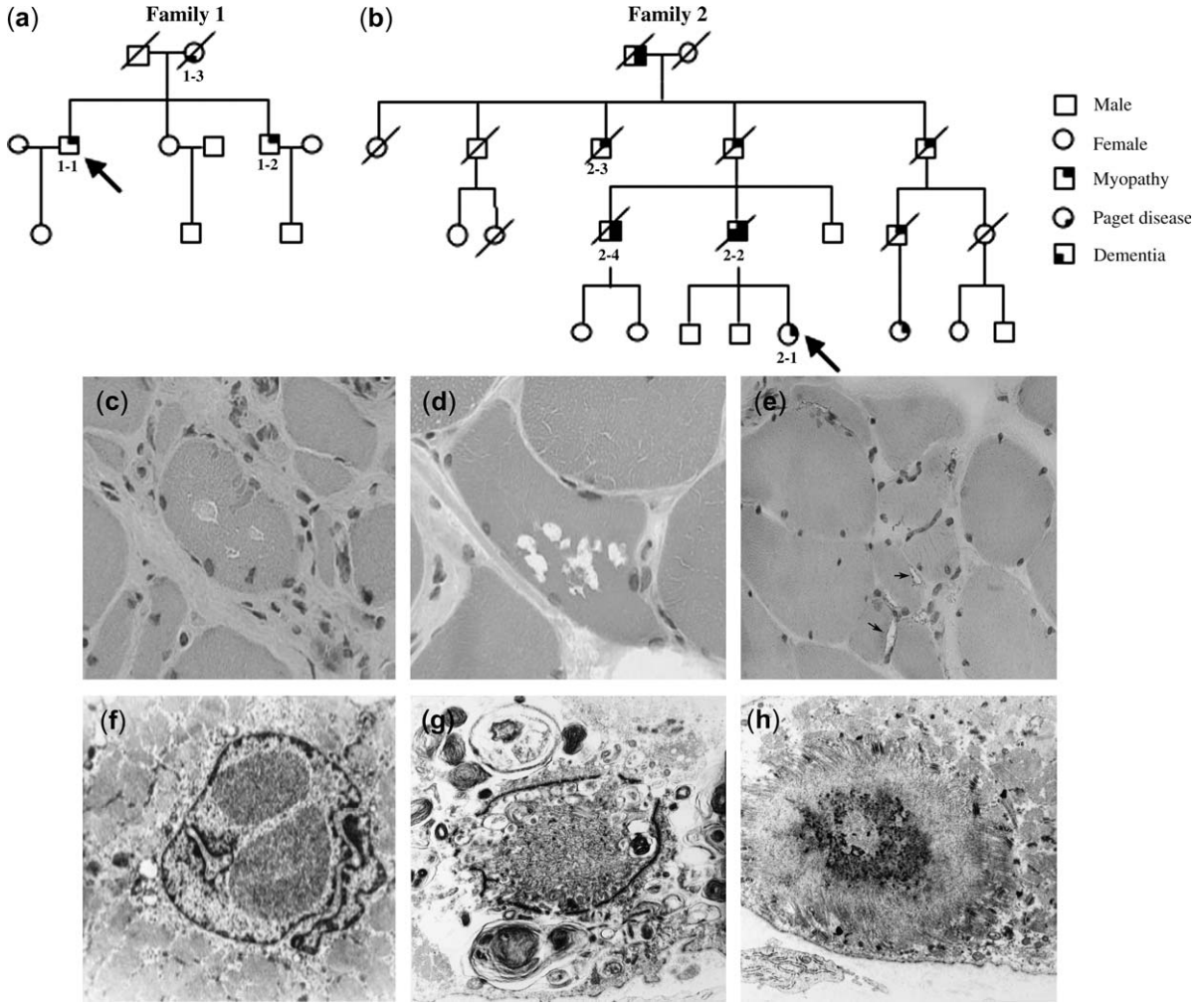

Fig. 1. (**a**) Pedigree of family 1 and (**b**) family 2, arrows indicate proband, and symbols with a slash indicate deceased individuals. (**c**) Light microscopy and electron microscopy (EM) of affected muscle. Individual 1-1 H-E × 400: rimmed vacuoles with eosinophilic inclusions, (**d**) Individual 1-2 H-E × 400: Vacuolar changes, (**e**) Individual 2-1 Congo red staining of right deltoid demonstrates myopathic changes with variation in fiber size and basophilic rimmed vacuoles in several muscle fibers (arrows). Magnification is 40×. (**f**, **g**) Individual 1-1 EM × 10,000: intranuclear inclusions in degenerating myonucleus, (**h**) muscle EM (×6000) of individual 1-1 shows cytoplasmic body.

records were obtained for some of the deceased affected individuals. There is a clear autosomal dominant family history of myopathy with two instances of PDB and one instance of FTD in the father of the proband who had all three major manifestations of the VCP related disease.

Case 4

Individual 2-1, the proband, a 36-year-old woman had a 1-year history of right arm weakness, inability to raise her arms above shoulder level, and pain in the lower neck, shoulder blades and right lower back. She had weakness of her limb-girdle muscles and marked scapular winging. Distal muscles were strong. Tendon reflexes are present bilaterally. Right deltoid muscle biopsy findings were consistent with an inclusion body myopathy. [Fig. 1(**e**)].

Case 5

Individual 2-2, the proband's father, who died at age 52 year developed increasing proximal weakness in both legs and arms at age 37 years, followed by foot drop a year later. Atrophy of the scapular muscles causing winging was noted. A biopsy of the quadriceps muscle showed evidence of advanced chronic myopathy with considerable fatty infiltration, focal inflammation, and many fibers with rimmed vacuoles. By age 44 years, he lost his ability to ambulate and was confined to the wheelchair. A bone scan at age 49 years was indicative of PDB.

At age 50 years, he was diagnosed with global dementia. Detailed neuropsychological examination for mild memory and associated cognitive problems revealed impairment on the Boston Naming test indicative of dysnomia, difficulties

on a number of verbal measures from the Wechsler Adult Intelligence Scale-R, difficulties with rate of learning and retrieval. His Full Scale IQ (FSIQ) was 99, verbal IQ (VIQ) 93 and performance IQ (PIQ) 111. His neuropsychological status was re-evaluated in 9 months, and dramatic deterioration was detected, characterized by his decline in VIQ = 72, PIQ = 79 and FSIQ = 79. He also displayed clear aphasic symptoms, significant anomia, further worsening of short-term memory and executive functions, irritability and confusion. His cognitive, behavioral and language decline progressed over the following 2 years, while hostility and aggression increased. Magnetic resonance imaging of the brain was unremarkable, single photon emission CT showed mild diffuse frontal lobe hypoperfusion. At age 50 years, left ventricular hypertrophy also was noted on electrocardiographic examination. His status further deteriorated, he was unable to move his limbs and hold his head up against gravity, developed difficulty swallowing, stopped using his wheelchair and was bedridden. His speech gradually decreased and finally regressed into mutism.

Postmortem examination of several muscle groups identified severe fatty infiltration and end stage atrophy of the lower extremity musculature with evidence of rimmed vacuoles, variation in fiber size, atrophic fibers suggestive of denervation atrophy. Postmortem electron microscopy of muscle sections confirmed the presence of rimmed vacuoles, and further revealed subsarcolemmal aggregates of membranous cytoplasmic bodies, tertiary lysosomes, swollen mitochondria, and scattered aggregates of straight filaments measuring 13–19 nm in diameter near the membranous bodies.

Postmortem neuropathological examination of the cerebral cortex showed prominent microvacuolation in the cortical layers with some thinning of the cortical ribbon. Cortical degeneration was most severe in the temporal and hippocampal region followed by the frontal lobe and minimally in the occipital lobe. Additionally, the spinal cord showed a decreased number of anterior horn cells, shrinkage of these cells with amorphous material within the cytoplasm, gliosis, and shrunken anterior roots in the lumbar and low cervical segments. Detailed microscopic studies, performed for this report by Forman et al. (10) on a brain autopsy sample obtained more than 10 years ago revealed dystrophic neurites and neuronal intranuclear inclusions both ubiquitin-positive that were not detectable with antibodies to tau, alpha-synuclein, beta-amyloid, neurofilament and polyglutamine repeats. The ubiquitin pathology was most abundant in the superior/middle temporal gyrus, followed by frontal and occipital lobes. A few neurofibrillary tangles were marked in the limbic structures.

We were unable to obtain detailed medical information on individual 2-3 (case 6), the deceased uncle of 2-2 who died at age 58 years from respiratory and cardiac failure or on individual 2-4 (case 7), the affected sibling of individual 2-2 who died of cardiac failure at age 57 years.

Molecular studies

We sequenced exons 3, 5, and 6 of VCP (3) and when these exons were determined to be normal, the remaining 14 exons of VCP were sequenced. The newly identified mutations were checked against the National Center for Biotechnology Information SNP database (URL: //www.ncbi.nlm.nih.gov/projects/SNP), and we screened 180 additional control chromosomes by a combination of sequencing control genomic DNA and alignment of all human cDNA and EST sequences from the National Center for Biotechnology Information non-redundant database for exon 10 and by restriction digests for base changes in exon 6 to exclude polymorphisms.

Cosegregation studies

Restriction site mapping from polymerase chain reaction amplified genomic exon sequences was utilized to confirm that the mutation cosegregated with disease in the families containing mutation 593 T > G (family 30) which destroys an *Bst*NI restriction site.

Results

Mutation analysis

Genomic DNA sequenced from patients 1-1 and 1-2 in family 1 identified the novel transversion mutation c.1159A > C in exon 10 of VCP [Fig. 2(**a**)]. The mutation changes amino acid residue 387 from asparagine to histidine, shifting this residue from polar hydrophilic to positively charged hydrophilic. The p.N387H mutation is found in the α5 helix of the first AAA-ATPase domain (D1), which is outside of the catalytic site of this domain.

Sequencing of DNA from individual 2-1 in family 2 identified the novel transversion mutation c.593T > G in exon 6 of VCP [Fig. 2(**b**)] that changes amino acid residue 198 from leucine to tryptophan (p.L198W). Although both amino acids are non-polar hydrophobic, the difference in size is significant. Thus, this mutation potentially

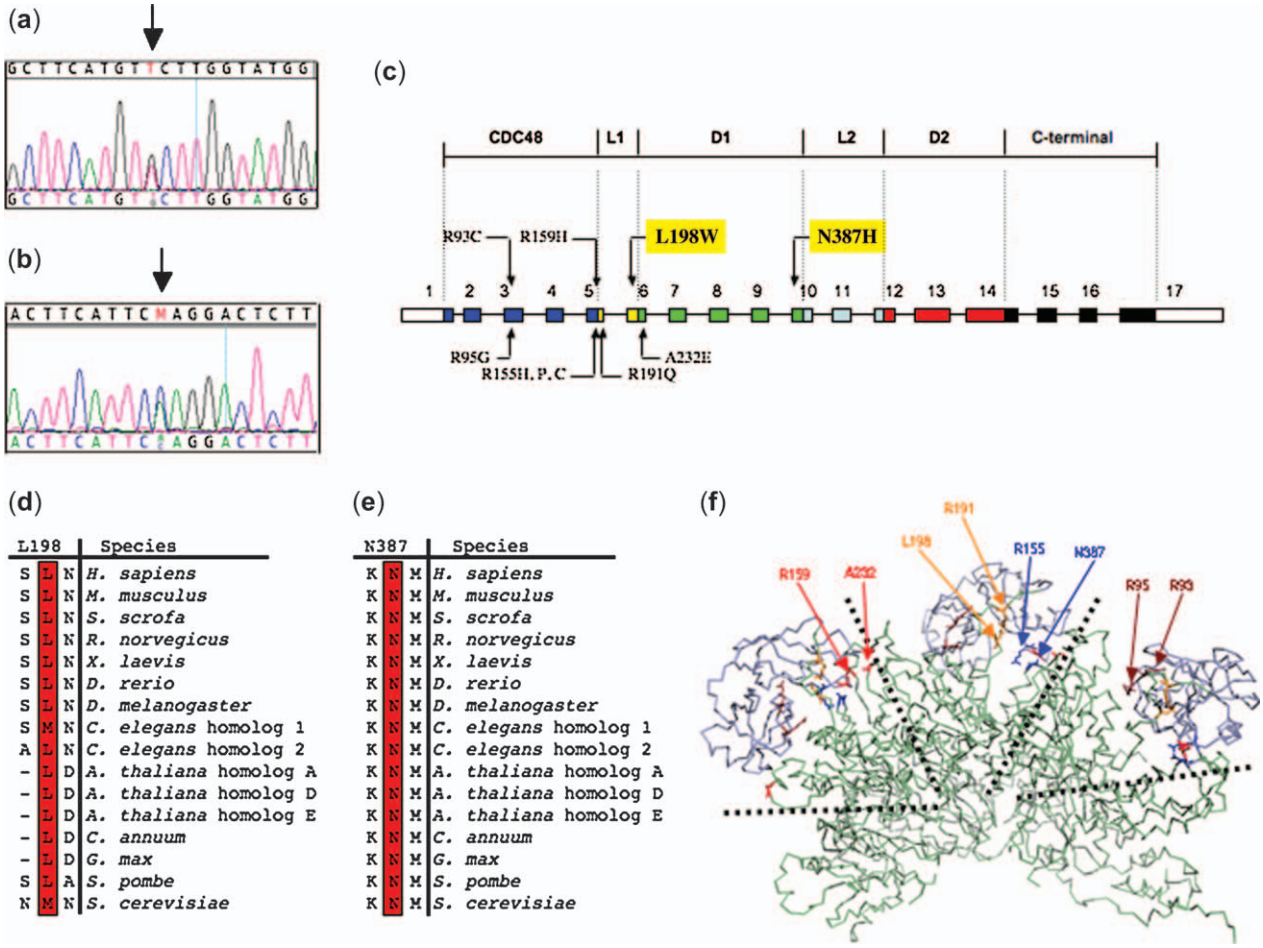

Fig. 2. Sequencing chromatograms of genomic DNA from each family. As IBMPFD is dominant, both chromatograms show two overlapping peaks at the mutant locus. (**a**) Family 1 and (**b**) family 2. (**c**) Functional domains and mutations in valosin-containing protein (VCP) in individuals with IBMPFD. Arrows indicate the locations of mutations relative to the exon–intron structure where the exons are numbered 1–17. The relative positions of the N-terminal domain (CDC48, dark blue), flexible linker (L1, yellow), first AAA-ATPase domain (D1, green), linker region (L2, light blue), second AAA-ATPase domain (D2, red) and C-terminal domain (black) are indicated, and the 5′ and 3′ untranslated regions are shown in white. Novel mutations are shown in red. (**d**, **e**) Alignment of the VCP amino acid sequence in various species in the p.L198W and p.N387H mutations region (**d** and **e,** respectively). The amino acid residues L198 and N387 mutated in IBMPFD are highly conserved among species (highlighted in red). (**f**) Structural context of IBMPFD mutations in VCP. A ribbon representation depicting the crystal structure of the VCP hemi-homohexamer (13)]. CDC48 domain is colored lilac and the remainder of the protein is colored pale green. Amino acid residues that are mutated in IBMPFD are colored brown, orange, dark blue and red, where residues of the same color are predicted to interact with one another in the *wt* protomer. These mutated residues also show the side chains for the *wt* amino acid. The dotted black lines represent the approximate protomer boundaries of a top down view of the protomer complex. The predicted interactions are either through direct side chain to side chain or side chain to backbone carbonyl group, for R155+N387, R159+A232 and R191+R198. The mutations R159 and A232 affect the adjacent VCP protomers. Residues R93 and R95 are located in a hydrophilic pocket within the double ψ barrel region of the CDC48 domain.

has structural implications because of its location in the first linker domain (L1).

Discussion

There are now 10 different familial mutations in VCP that have been associated with IBMPFD: p.R93C, p.R95G, p.R155C, p.R155H, p.R155P, p.R159H, p.R191Q, p.L198W, p.A232E, and p.N387H. More than half of these mutations cluster in the N-terminal CDC48 domain, two affect the first linker domain, and two are found in the first AAA-ATPase domain [Fig. 2(**c**)].

VCP is highly conserved among species, and the amino acid residues in which we found the novel p.L198W and p.N387H mutations are likewise highly conserved [Fig. 2(**d**, **e**)]. Despite their differences in location, p.L198W and p.N387H may

in fact have a similar consequence. The substitution of tryptophan for leucine in amino acid residue 198 (p.L198W) in the first flexible linker may affect or inhibit normal movement of the N-terminal. This in turn can have an effect on changes in the N-terminal conformation, thus potentially affecting binding interactions within this domain. By placing all of the published IBMPFD mutations onto the 3D structure, we see a very particular spatial clustering of affected amino acid residues, where most seem to form interacting pairs. When these mutations are placed in the context of the 3D protein structure [Fig. 2 (**f**)], we find that they are clustered in the region of the interface between the CDC48 N-domain with the D1-ATPase domain. Significantly, most of the mutated residues are adjacent and potentially interact with each other (R155-N387, R159-A232 and R191-L198), suggesting that these residues may have a similar and specific function within the VCP homohexamer. Residues R155, R159 and N387 may form a significant interaction depending on the ATP hydrolysis states of D1 and D2, forming a stable conformation locking the CDC48 domain down. Additionally, the backbone carbonyl group of residue R159 may also interact with the side chain of N387. The mutations R93 and R95 are both located in the double ψ barrel (amino acids 25–106) region of the CDC48 domain and while they do not seem to directly interact, they are part of a hydrophilic region formed by the double ψ barrel, the four-stranded β barrel (amino acids 112–186) and the flexible linker region (amino acids 187–208) that connects the CDC48 domain to the D1-ATPase domain. Mutations in either of the residues would affect the potential ligand binding properties of this region. Using a virtual screen of ligand databases Hübbers et al. (11) predicted that this R93-R95 region could potentially bind cyclic sugar moieties, and speculated that this region could be implicated in the binding of carbohydrates from misfolded glycoproteins in the endoplasmic reticulum (another function of VCP (12)), and the R93 or R95 VCP mutations would potentially disrupt this function.

This would imply that VCP mutations that cause IBMPFD are very specific within the structural context of the protein and must define a physiologically specific function. Delineation of the functional changes in VCP caused by these mutations will provide some insight into the pathogenesis of this debilitating multi-system disease.

Acknowledgements

We thank the families and their health care providers for their enthusiastic participation and contribution in our research studies. We thank Mark Forman for detailed histopathological studies on autopsy material. Funding of this study is from the National Institute of Arthritis and Musculoskeletal and Skin Diseases, National Institutes of Health (R03 AR 46869, R01AR050236), Muscular Dystrophy Association and Paget Foundation.

References

1. Kimonis VE, Kovach MJ, Waggoner B et al. Clinical and molecular studies in a unique family with autosomal dominant limb-girdle muscular dystrophy and Paget disease of bone. Genet Med 2000: 2 (4): 232–241.
2. Kovach MJ, Waggoner B, Leal SM et al. Clinical delineation and localization to chromosome 9p13.3-p12 of a unique dominant disorder in four families: hereditary inclusion body myopathy, Paget disease of bone, and frontotemporal dementia. Mol Genet Metab 2001: 74: 458–475.
3. Watts GD, Wymer J, Kovach MJ et al. Inclusion body myopathy associated with Paget disease of bone and frontotemporal dementia is caused by mutant valosin-containing protein. Nat Genet 2004: 36 (4): 377–381.
4. Hetzer M, Meyer HH, Walther TC, Bilbao-Cortes D, Warren G, Mattaj IW. Distinct AAA-ATPase p97 complexes function in discrete steps of nuclear assembly. Nat Cell Biol 2001: 3 (12): 1086–1091.
5. Rabinovich E, Kerem A, Frohlich KU, Diamant N, Bar-Nun S. AAA-ATPase p97/Cdc48p, a cytosolic chaperone required for endoplasmic reticulum-associated protein degradation. Mol Cell Biol 2002: 22 (2): 626–634.
6. Rabouille C, Kondo H, Newman R, Hui N, Freemont P, Warren G. Syntaxin 5 is a common component of the NSF- and p97-mediated reassembly pathways of Golgi cisternae from mitotic Golgi fragments *in vitro*. Cell 1998: 92 (5): 603–610.
7. Zhang X, Shaw A, Bates PA et al. Structure of the AAA ATPase p97. Mol Cell 2000: 6: 1473–1484.
8. Guyant-Marechal L, Laquerriere A, Duyckaerts C et al. VCP mutations in two kindreds with prominent frontotemporal dementia: clinical and neuropathological features. Neurology 2006: 67: 644–651.
9. Haubenberger D, Bittner RE, Rauch-Shorny S et al. Inclusion body myopathy and Paget disease is linked to a novel mutation in the VCP gene. Neurology 2005: 65 (8): 1304–1305.
10. Forman MS, Mackenzie IR, Cairns NJ et al. Novel ubiquitin neuropathology in frontotemporal dementia with VCP gene mutations. J Neuropathol Exp Neurol 2006 65: 571–581.
11. Hübbers CU, Clemen CS, Kesper K et al. Pathological consequences of VCP mutations on human striated muscle. Brain 2007: 130: 381–393.
12. Yoshida Y, Adachi E, Fukiya K, Iwai K, Tanaka K. Glycoprotein-specific ubiquitin ligases recognize N-glycans in unfolded substrates. EMBO Rep 2005: 6: 239–244.
13. DeLaBarre B, Brunger A. Nucleotide dependent motion and mechanism of action of p97/VCP. J Mol Biol 2005: 347: 437–452.